UNIVERSITÀ POLITECNICA DELLE MARCHE

DIPARTIMENTO SCIENZE DELLA VITA E DELL'AMBIENTE

Corso di Laurea Magistrale

Biologia Molecolare e Applicata

Caratterizzazione di un transistor ad effetto di campo a grafene per il rilevamento di SARS-CoV-2

Characterization of graphene field effect transistor for SARS-CoV-2 detection

Tesi di Laurea Magistrale
di:

Gianmarco Melone

Relatore
Chiar.mo Prof.

Daniele Di Marino

Correlatore: (se previsto)

Anna La Teana

Correlatore: (se previsto)

Mattia D'Agostino

Sessione straordinaria

Anno Accademico 2019/2020

Index

Caratterizzazione di un transistor ad effetto di campo a grafene per il rilevamento di SARS-CoV-2

L'attuale quadro pandemico ha posto, senza alcuna ombra di dubbio, grande attenzione su "SARS-CoV-2", da parte dell'intero mondo scientifico. Il quadro generale si è andato delineando a partire dal Dicembre 2019, quando cioè molte strutture sanitarie in Wuhan (Cina) hanno riportato numerosi casi di pazienti con polmoniti da cause sconosciute. Ben presto si è compreso come i sintomi associati a tali polmoniti, quali febbre, tosse, dolore toracico ed in molti casi dispnea erano correlati ad infezioni da parte di membri del gruppo dei Coronavirus (CoVs). In termini generali, a questo gruppo appartengono virus dotati di envelope con un genoma a RNA a singolo filamento positivo che sono classificati in quattro generi: Alphacoronavirus, Betacoronavirus (al quale appartiene SARS-CoV-2), Gammacoronavirus e Deltacoronavirus. La grave situazione ha messo in evidenza l'estrema necessità di avere a disposizione metodi che permettano in maniera altamente specifica ed efficiente l'identificazione del SARS-CoV-2 al fine di arginare e limitare l'infezione su scala pandemica.

Lo scopo di questa tesi è stato quello di sfruttare le straordinarie proprietà e caratteristiche chimico-fisiche del grafene e più precisamente di un transistor ad effetto di campo (o FET) costituito da grafene per costruire un sensore che permetta di eseguire una rapida ed affidabile identificazione di SARS-CoV-2. Il transistor ad effetto di campo a grafene è rappresentato da un chip di silicio commerciale (Graphenea ®) su cui due elettrodi in metallo (source e drain) permettono il passaggio di corrente su un monostrato di grafene; un terzo elettrodo definito gate regola il flusso di elettroni.

Per il progetto di questa tesi abbiamo deciso di utilizzare e caratterizzare tre differenti biorecettori: i) Il recettore ACE2 che rappresenta il bersaglio naturale della proteina virale Spike (in particolare del suo dominio RBD); ii) l'anticorpo anti-Spike; iii) la molecola chimerica Fc-ACE2 contenente il frammento anticorpale Fc legato alla proteina ACE2. Le tre proteine verranno inizialmente ancorate sulla superficie di grafene sfruttando il linker pirenico PBASE, ampiamente usato nel campo della biosensoristica. Il linker sarà in grado di esplicare la propria attività di "ponte molecolare" interagendo da un

lato con il foglio di grafene e dall'altro, grazie ai suoi gruppi funzionali tramite coupling peptidico con una proteina di interesse.

L'aspetto chiave degli esperimenti condotti risiede nel fatto che l'interazione tra le proteine fissate sul grafene e la proteina Spike causerà una variazione nella corrente che attraverserà il GFET e l'interpretazione di questo segnale è alla base dell'applicazione di tale tecnologia per lo scopo designato.

In particolar modo i risultati ottenuti si sono basati sull'osservazione nella variazione dell'intensità di corrente (I) e della resistenza (R, Ohm). Il punto principale era quello di osservare variazioni in uno di questi ultimi due valori, da interpretare quindi come segno di interazione tra le due proteine.

Tutti e tre questi risultati hanno mostrato considerevoli variazioni in intensità di corrente (o resistenza), ma il risultato che ha mostrato una più netta variazione risulta essere quello ottenuto con la molecola chimerica Fc-ACE2.

Le ragioni di questo risultato stanno alla base di un aspetto essenziale riguardante il processo di funzionalizzazione, ovvero il corretto orientamento spaziale della molecola ACE2 sulla superficie del grafene. L'utilizzo

degli anticorpi anti-Spike ha mostrato ottimi risultati essendo questi, estremamente specifici nell'interazione con la proteina Spike. La variazione in chiave di misurazione di corrente è risultata più netta rispetto al solo ACE2. I risultati più netti ottenuti con l'utilizzo della molecola chimerica Fc-ACE2 hanno quindi sfruttato i vantaggi dati da un miglior orientamento spaziale sulla superficie del grafene essendo in questo caso il frammento Fc a prendere contatto con la superficie e non ACE2 stesso, ma allo stesso tempo sfruttando la naturale interazione tra ACE2 e Spike, simulando così quanto avviene nel corso di un'infezione da SARS-CoV-2.

In conclusione, tutte e tre le molecole utilizzate hanno prodotto una variazione rilevante nell'intensità di corrente, ma le variazioni più nette sono state ottenute tenendo conto di una migliore disposizione del target molecolare designato sulla superficie del grafene. Dopo la valutazione di questi vari e differenti aspetti in merito ai risultati ottenuti, si prefigura tra l'altro, la futura possibilità di implementazione di tale tecnologia simulando tramite un film lipidico quello che è il natural environment di ACE2 garantendone così,

essendo un recettore integrale di membrana, un corretto ed adeguato orientamento spaziale senza la necessità di utilizzare linker sulla superficie del grafene. Un altro interessante prospetto sembra essere anche, al fine di evitare interazioni dirette tra ACE2 e la superficie del grafene, linker con lunghe code apolari la cui forza di interazione sulla superficie del grafene sarà proporzionale alla lunghezza della coda stessa data la natura delle interazioni in gioco e che permettano così di creare delle ordinate batterie di linker che assicurino una regolare e corretta disposizione spaziale di ACE2 sul grafene.

First chapter

INTRODUCTION

1.1 Notes on SARS-CoV-2 and worldwide spread

The actual pandemic emergence that has involved the entire world has given, of course, much importance to "SARS-CoV-2". Starting from December 2019, many hospitals in Wuhan (China) have reported several cases of patients with a particular pneumonia of an unknown origin (1). In a similar way to patients afflicted by the famous SARS and MERS, these patients showed symptoms of viral pneumonia, with fever, cough, chest pain and in many cases, dyspnea, in addition to bilateral pulmonary infiltration (2) (3). Frequently, these symptoms are associated to an infection caused by memebrs of Coronavirus group (CoVs). In general, this group includes viruses with an *envelope* and a genomic single postive strand RNA (4). They are typically classified in 4 genera: *Alphacoronavirus, Betacoronavirus, Gammacoronavirus and Deltacoronavirus*. As new *Betacoronavirus*, SARS-CoV-2 shares the 79% of genomic sequence identity with SARS-CoV and the 50% with MERS-CoV (5); the general organization of its genome is shared with other members of *Betacoronavirus* genus. It is possible to identify six functional open reading frames (ORFs) in 5'-3'direction: -Replicase (ORF1a/ORF1b), -Spike (S), -Envelope (E), -Membrane proteins (M), -

Nucleocapsid (N), but seven additional putative ORFs were identified, interspersed between structural genes (6). Most of the protein coded by SARS-CoV-2 have a similar length with the corresponding SARS-CoV's proteins sharing over 90% identity except for the Spike protein that is quite different (7,8). Firstly, the SARS-CoV-2 Spike protein is composed by 1273 aminoacids, longer than SARS-CoV's Spike (1255 amminoacids) "Bat SARSr-CoVs" (1245- 1269 aminoacids). Secondly, it is much different also compared with Spike protein of many members of Sarbecovirus subgenus (*Betacoronavirus* genus) (9). Spike protein will play a key role for the cell invasion and once the virus enters inside the cell, its cycle consists in the expression and replication of its own genomic RNA for the production of several genomic copies. The 5' and 3' *untranslated regions* that form secondary *cis-acting* structures play a key role for the RNA replication. More specifically about the role of Spike protein, it is important to understand that in the receptor-binding domain (RBD) of Spike protein(S), the aminoacidic sequence similarity between SARS-CoV-2 and SARS-CoV it is just of 73%. (10). SARS-CoV-2 uses the same receptor of SARS-CoV, the "angiotensin-converting enzyme 2" (ACE2) (11) (12). The S1 subunit of Spike protein (S) is divided in two functional domains, the N-terminal domain and the C-terminal domain; in this last domain biochemical and structural analysis have

identified a 211 aminoacids region (319-529), known as RBD (receptor binding domain), with a key role for cell invasion and which also represents the main antibody target (13) (14). In particular, it is possible to identify, inside the RBD, a receptor-binding motif (RBM, amminoacids 437-507) that provides, specifically, the contact with ACE2 and it differs from SARS-CoV's RBM in five critical residues (Y445L, L486F, N493Q, D494S, e T501N) (15). These different aminoacids establish a more stable interaction between SARS-CoV-2 and its receptor, in particular the interaction stability increases in the two "viral hotspots" present in the human ACE2 (hACE2) (16). In addition, a four residues motif in SARS-CoV-2's RBM (aminoacids 482-485: G-V-E-G) is responsible of an interaction with the N-terminal region of hACE2, with a higher affinity with respect to SARS-CoV (17). Biochemical analyses have confirmed that these structural modifications in SARS-CoV-2's RBD have reinforced the binding affinity with hACE2, differently from what happens in SARS-CoV (18) (19) (20). Spike protein that, as it was told before, presents particular characteristics that make it different from SARS-CoV's Spike, but in general from the Sarbecovirus' Spike. In addition, it is possible to highlight Spike's importance considering its role for the invasion of the target cell. Spike is an homotrimeric glicoprotein and every single monomer is formed by two subunits, S1 and S2.

The interaction of Spike protein with ACE2 causes a series of cascade events necessary for the virus entry. The initial interaction between ACE2 and Spike induces an S2 subunit dissociation from ACE2 itself, but it is necessary for the S2 transition from a "pre-fusion" state to a more stable "post-fusion" state that is essential, as the name suggests, for the fusion of target cell membrane with the envelope (21) (22) (23) (24). The role of S2 subunit is important for cell invasion, but also S1 has a big importance with its RBD domain, a key element for the initial interaction with ACE2 (25) (26). Another important element is represented by ACE2 that is the Spike's target; in fact it was observed that HeLa cells with an active expression of ACE2 have a complete susceptibility for SARS-CoV-2 infection; on the other hand HeLa cells without the expression of ACE2 weren't susceptibles for SARS-CoV-2 infection (27). In particular, SARS-CoV-2 RBD has a β-sheet formed by five antiparallel strands (β1, β2, β3, β4, β7) with small helices and loops that act as connection in a structure defined RBD's core. (Figure 1)

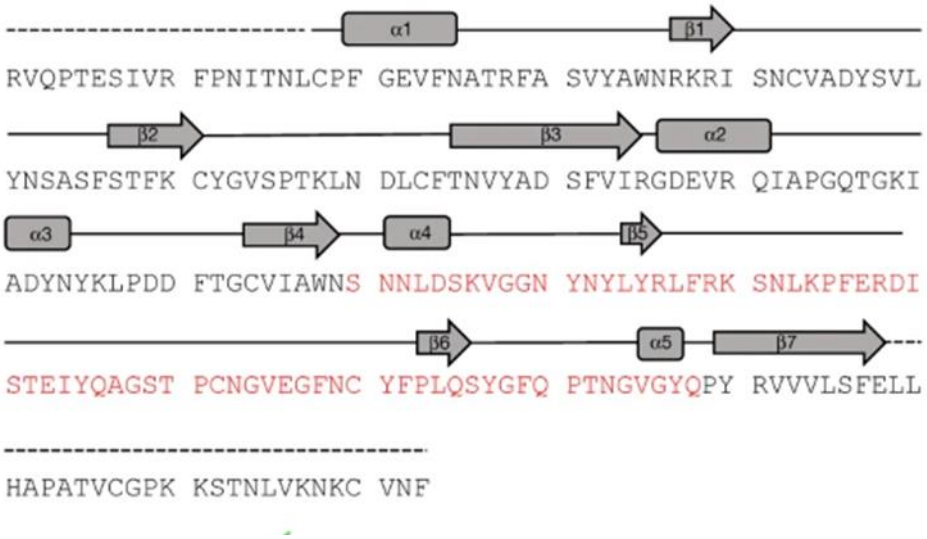

(Figure 1) (Sequence and secondary structure of SARS-CoV-2's RBD. RBM is showed in red)

Between β4 and β7 strands inside the core, there is an extention with a typical insertion that contains β5 and β6 strands, loops and the α4 and α5 helices; this extended insertion represents the RBM. It contains the main residues involved in the interaction with ACE2. Inside RBD were found nine cysteine residues, eight of them form four disulphide bonds that contribute to the stability of this domain because three of these four disulphide bonds are present in the core and the last one is in the distal portion of RBM. For what concerns ACE2, the N-terminal peptidase domain presents two lobes where, in the space between them, is possible to find the substrate binding site. The RBM interacts with the lower portion of these two lobes and with the help of RBM's external concave surface, the binding with ACE2's N-terminal helix happens. (Figure 2)

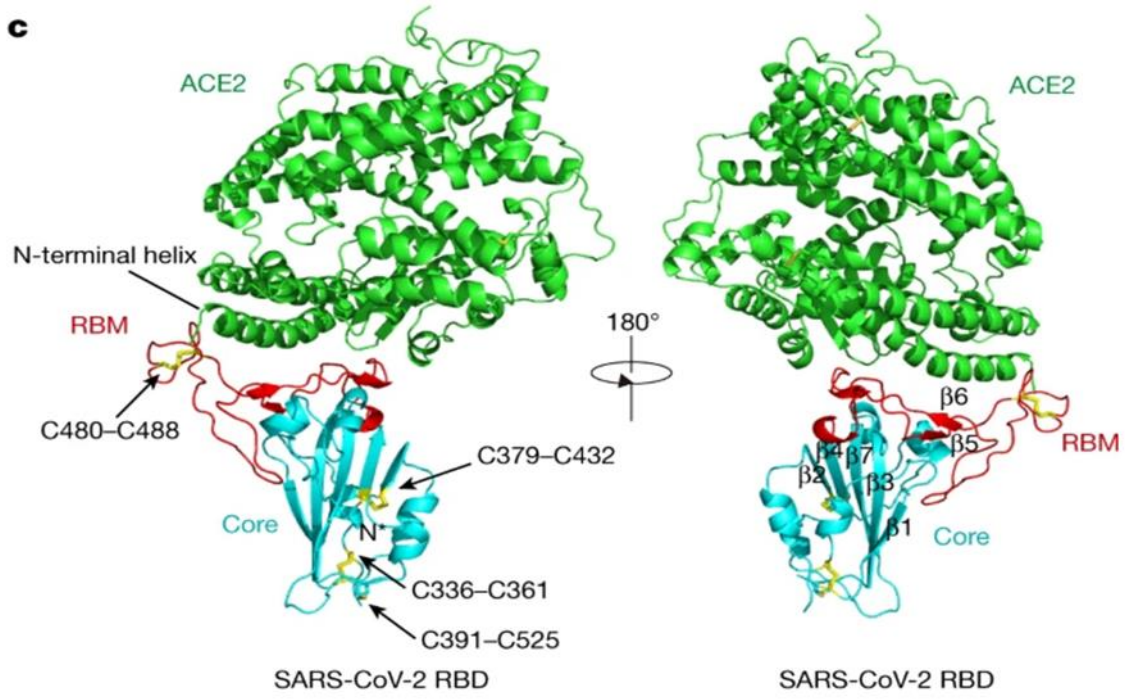

(Figure 2) (SARS-CoV-2's RBD bound with ACE2. RBD's disulphide bonds indicateb by arrows and represented as "sticks")

Briefly, Spike protein is essential for cell invasion because it is an homotrimeric fusion glicoprotein divided into two essential functional subunits, the S1 and the S2 subunits. As mentioned above RBD domain is located inside S1 subunit, but at the same time it is really important the transmembrane domain in the S2 subunit that contains the fusion peptide, that, in particular, mediates the fusion between the cellular membrane and the viral envelope as a consequence of structural rearrangments (28) (29) (30). These Spike's features are important element for the SARS-CoV-2 detection. The diagnostic methods used are divided in two categories: 1) molecular tests that detect the presence of viral genomic RNA, 2) rapid tests or antigen tests that detect the presence of a viral antigen. With the rapid development of

technology in the biosensing field another method can be added, the graphene Field Effect Transistor (GFET) SARS-CoV-2 detection. In consideration to this new perspective the aim of the project was to set up a clear, cheap, fast and highly reliable method for the SARS-CoV-2 detection.

1.2 Chemical-physical characteristic of a GFET

In general, a typical Field Effect Transistor is a semiconductor channel with electrodes at either end referred to as the drain and the source. A control electrode called the gate is placed in very close proximity to the channel so that its electric charge is able to affect the channel. In this way, the gate of the FET controls the flow of carriers (electrons or holes) flowing from the source to drain. It does this by controlling the size and shape of the conductive channel. With this great characteristics and advantages showed it can be really useful for an actual global challenge like SARS-CoV-2 the use of field effect transistor technology. Considering the characteristics of this interaction and the high specificity showed for ACE2 by SARS-CoV-2's Spike protein, the application and the use of GFET for the diagnosis of SARS-CoV-2 infection becomes really useful and with a high potential. The possibility to use ACE2 as an immobilized target on these GFET guarantees a fast response and a good reliability. In particular, GFET (graphene Field Effect Transistor) uses the extraordinary properties of grafene that make it really useful in different

scientific fields, in particular the biotechnology and nanotechnology ones. For our project, the use of this kind of technology is based on thin graphene sheets inserted in a chip with a thickness of 675 μm with a total capability of 12 graphene sheets for a single chip (Graphenea ®) (31) (Figure 3); the sp^2 hybridization of graphene's carbon orbitals plays an essential role in the determination of its most relevant chemical-physical properties that are used for the GFET application. The extended electron delocalization of π orbitals creates a continue system for all the graphene sheet surface with the formation, on this way, of a big *electron delocalization's cloud* that results higly accessible for linker molecules with aromatic chains or with long apolar chains that interact with *π-stacking, hydrophobic effect* and in general, with *Van Der Waals interactions*. According to this kind of interactions on the graphene's surface clearly results that these aren't covalent interactions; for this reason the interaction's strenght will be minor than a classical covalent bond even if the possibility of linker use with long apolar chains increases the strenght of this non-covalent bond because on this way the bond's strenght increases proportionally with the lenght of apolar chain itself. This gives the possibility to create regular series of linker on the graphene's surface and this aspect will permit the next step of functionalization, a highly controlled density and position of the receptor ACE2. For what concerns the use of a

typical GFET, the measurements are made with the simultaneous application of two different kind of voltage: the source-drain voltage (V_{SD}) that passes between the two electrodes (source and drain); the V_{SD} permits the movement of electrical charge through the graphene that is associated with a source-drain current (I_{SD}) with the possibility to change the voltage V_{SD} to obtain the desired I_{SD}. It is also essential for the measure, the gate current (or gate voltage) that can be applied on the silica layer from the back (back gating) with the help of a thin diamond needle that scratches the 90 nm thickness of silica's surface (Graphenea®) from one of its angles. The current variation between source and drain, according to what it was reported before, is the main signal to consider in biosensing; this is in fact, a critical event of possible target detection (32).

(Figure 3) (Chip Graphenea®, total dimensions 10mm x 10 mm)

1.2.1 Biotechnological applications

According to these important characteristics that make GFET very useful, it is obvious that there's a big use in biotechnological and nanotechnological field, it can be considered as a revolutionary tecnique for these sectors. There are various applications possibility in many different fields, from the ecology to the detection of toxic pesticides in cultivations, but the most important application is the medical one. Some important examples in this last sector show how much important biosensors are becoming for the human health. A very important example is the detection of choleric toxin in contamined lake water samples (33). Other examples of high impact are the rapid detection of carbofuran, a well known neurotoxin (34), the identification of the α-emolisin whose presence is typically associated to *Staphylococcus aureus* infections (35) (36), another important example is, the human papilloma virus detection even if it is slightly different in this case because the target is the virus' DNA (37). The huge use of GFET for the medical field makes biosensors a highly impact tecnology; there are many advantages, but the most important are a fast response time (in some cases less than five minutes) and also the extreme sensitivity that a GFET shows, in fact it can detect really low concentrations of target with high precision and reliability.

1.2.2 GFET functionalization

Every single aspect on the basis of GFET functionalization requests the exact knowledge of graphene's chemical-physical properties, listed in the previous paragraphs. The extended electron delocalization due to the expanded π system on the top and on the bottom of the plane formed by graphene sheet contributes to the formation of this big electron cloud that gives to the graphene most of its principal properties. For the functionalization step it will be necessary the use of a linker as a "bridge molecule" between graphene and ACE2 that permits to anchor it on its surface.

1.2.3 Possible approaches for the functionalization

A typical linker needs specific properties that permit a good interaction with graphene; for this reason the use of molecules with aromatic chains represents a good option because they have the same electron delocalization system present in the graphene; 1-pyrenebutanoic acid succinimidyl ester (PBASE) results one of the most famous and applied linker for this reason. (Figure 4)

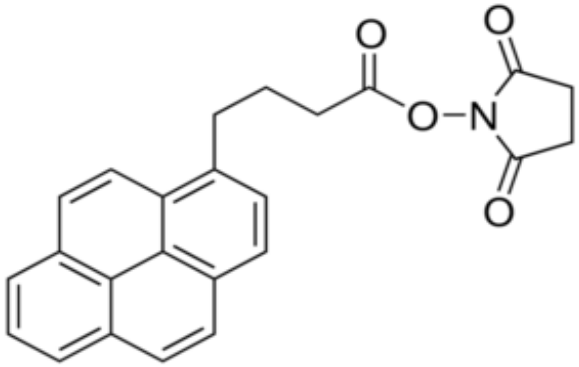

(Figure 4) (PBASE with its aromatic chain)

A good linker doesn't need only the faculty to interact in a good manner with the graphene, but it also needs the ability to bind (in this case) ACE2 to execute its activity of "bridge molecule" giving a good interface between graphene and ACE2. The binding with ACE2 happens, as it is possible to see in the image (Figure 4), with a *peptide coupling*, forming in this way, a covalent bond with ACE2. There are many other linker in addition to PBASE and different ways for the functionalization step. It is possible to use, for example, long apolar chains that mainly interact with *Van Der Waals interactions*. In this case the strenght interaction proportionally increases with the chain lenght forming a "carpet" of linker regulary distributed on the graphene's surface (38). Another alternative is the covering of the graphene sheet with a lipidic film, simulating in this way, the natural environment of ACE2 without the help of a linker (39). The main risk of the linker use is that they aren't covalently anchored to the graphene's surface and for this reason they can't guarantee a regular distribution of ACE2 receptor.

1.2.4 PBASE use and alternatives

PBASE is one of the most commonly used linkers in the biosensing sector and its aromatic chains are useful for the binding on graphene's surface. This is a large surface with a high electron delocalization; in addition, the possibility to bind ACE2 to PBASE with peptide coupling represents an

important aspect offered by this linker. The non-covalent binding between graphene's surface and PBASE doesn't permit a strong anchorage on graphene's surface with also the risk of irregular aggregates formation. For these reasons there are useful alternatives to PBASE that can be used. There are many possibilities to use linkers with different chemical-physical properties. One of these is the use of long apolar chain (hydrocarbon chains) as linker with Van Der Waals interaction on graphene's surface. The use of linkers isn't the only opportunity because this function of "molecular bridge" between graphene and ACE2 can be assolved by a lipidic film with the aim to build and simulate the ACE2's natural environment. In this way it is also possible a natural and regular folding of ACE2 on this lipidic film, with its transmembrane helix, ACE2, in fact, is a membrane receptor.

1.3 *AFM application for GFETs*

Once selected an adequate linker for the step of GFET's functionalization it is necessary monitoring the linker binding step trying to avoid a bad linker distribution on the graphene's surface. The linker binds to the surface with a non-covalent way; for this reason, there can be problems that can hinder the

outcome of the entire experiment. As said before, this isn't a covalent bond and considering the extended electron delocalization cloud on the graphene's surface itself, a linker formed with aromatic chains risks fluctuating on this electron cloud without a stable and permanent position because this kind of interactions, hydrophobic effect, Van Der Waals interactions and π-stacking are extended for all the graphene's surface and not in a specific point of its surface. This isn't the only risk, because without a fixed position of the linker there is the possibility to form aggregates between linker's aromatic chains causing not only a consequent unequal distribution of ACE2, but also the impossibility to covalently bind ACE2 to the linker itself because it is present in unregular aggregates. A good functionalization is the basis for a good result. For this reason the application of *atomic force miscroscopy* (AFM) is fundamental. This kind of microscopy permits to obtain (with the help of Lennard-Jones forces) images of sample's surface with high fidelity. For this task are usually used probe tips composed by silicon nitride or diamond because they must get in touch with sample's surface; exactly for this reason, materials with strenght and compactness are requested. Briefly, the reliefs on sample's surface cause forces that act on the tip of the needle deforming the support on which they rest causing the shift of angular radius on a reflecting surface anchored to the support; in this way it is produced a current

proportional to the force acting on the tip of the needle; this current it will be used for the construction of sample's surface image (40). With this particular kind of microscopy, it is possible to understand if there is a good distribution of the linker.

Chapter two

RESULTS

2.1 PBASE distribution

During the experiments we have used three different concentrations of PBASE (2,5, 5 and 10 mM). The AFM results show that the most regular distribution has been obtained using 5 mM of PBASE (1 mg of PBASE in 500 μL of Dimethylformamide (DMF)) (Figure 5); differently from the other two results showed in the images (Figures 6,7), in fact with 2,5mM of PBASE (1 mg of PBASE in 1 mL of DMF) (Figure 6) it is possible to observe a too low distribution; on the contrary with a PBASE concentration of 10 mM (1mg of PBASE in 250 uL of DMF) (Figure 7) the concentration results to much high, with a clear presence of linker aggregates and irregularities in the space. With the AFM application it was possible to understand which is the best concentration of PBASE.

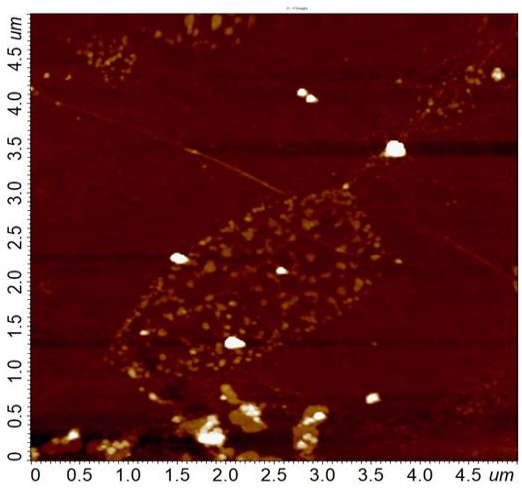

(Figure 5) (AFM graphene with PBASE 5 mM)

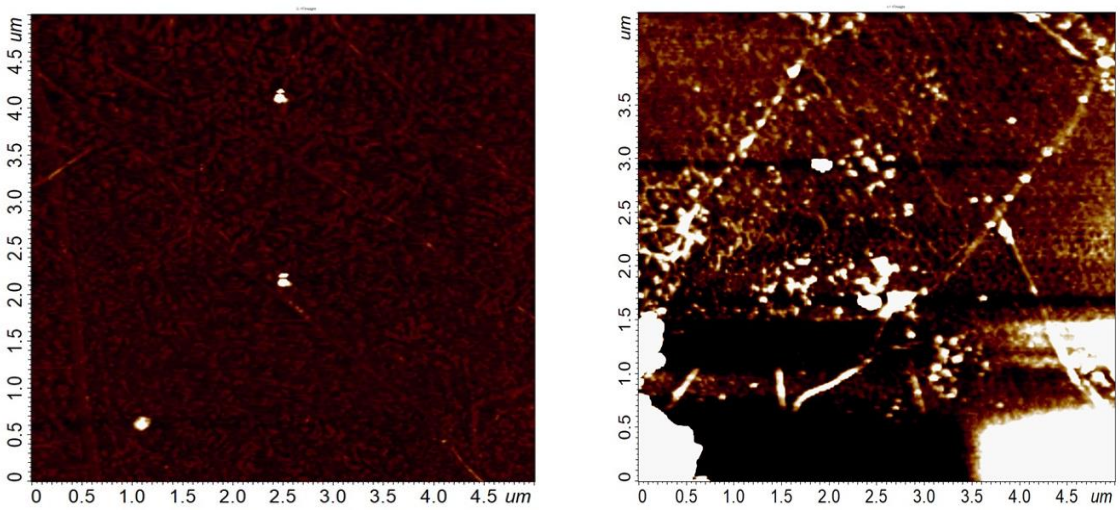

(Figures 6,7) (AFM graphene with PBASE 2,5 mM on the left, 10 mM on the right)

2.2 GFET electrical characterization using ACE2-His, Antibody against spike and Fc-ACE2 as bioreceptors.

The measurements have been done considering the V(g), that represents the gate voltage. The principal aim was to observe some variations in the V(g), because this could be clearly interpreted as an evidence of interaction between ACE2 and RBD resulting in a final variation of I or R (depending on the value considered). The current intensity I is inversely proportional to the resistance R (R=V/I); for this reason, the curves obtained have an opposite shape even if they have both the same task that consists in the observation of a current (or resistance) shift. Considering this, the measurements made for the negative controls play a key role because if there isn't a specific interaction with ACE2 (independently from the molecule used as negative control) consequently it shouldn't be observed any significant variation in the current intensity. In figure 8 it is possible to observe a schematic image of ACE2-His, the first recombinant version used as GFET bioreceptor.

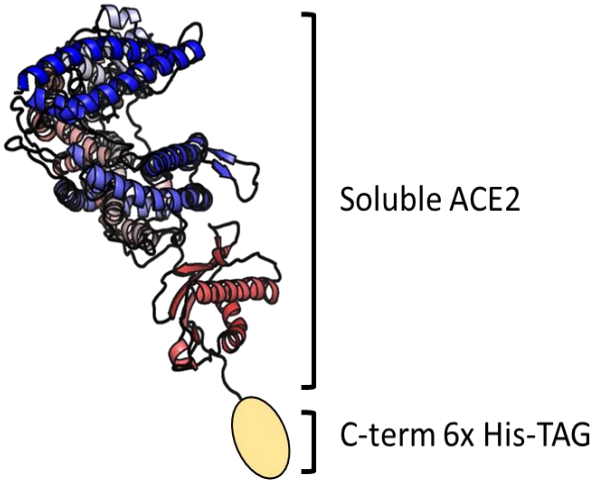

(Figure 8) Ribbon representation of ACE2-His used as bioreceptor

The figure 9B shows the current intensity in function of gate voltage V(g). It is important to observe a curve shift of Spike sample (represented in dark purple) from the blank (light purple). This curve shift can be considered as an interaction between Spike and ACE-His (anchored on graphene's surface). In the figure 9C it is possible to observe the same curve shift, but considering the resistance (R). The resistance is inversely proportional to the current and also in this case there is the same curve shift as for the current intensity and this represents a clear interaction between Spike and ACE-His. In the figure 9A, instead, it is represented the shift between the minimum point of V(g) in the peak (also known as Vdirac) and the blank (Spike). The same experiment has been done using mPRO as negative control (showed in the images 9 D,E,F). In this case the figure 9D shows that there isn't any Vdirac variation between

the blank and the sample.

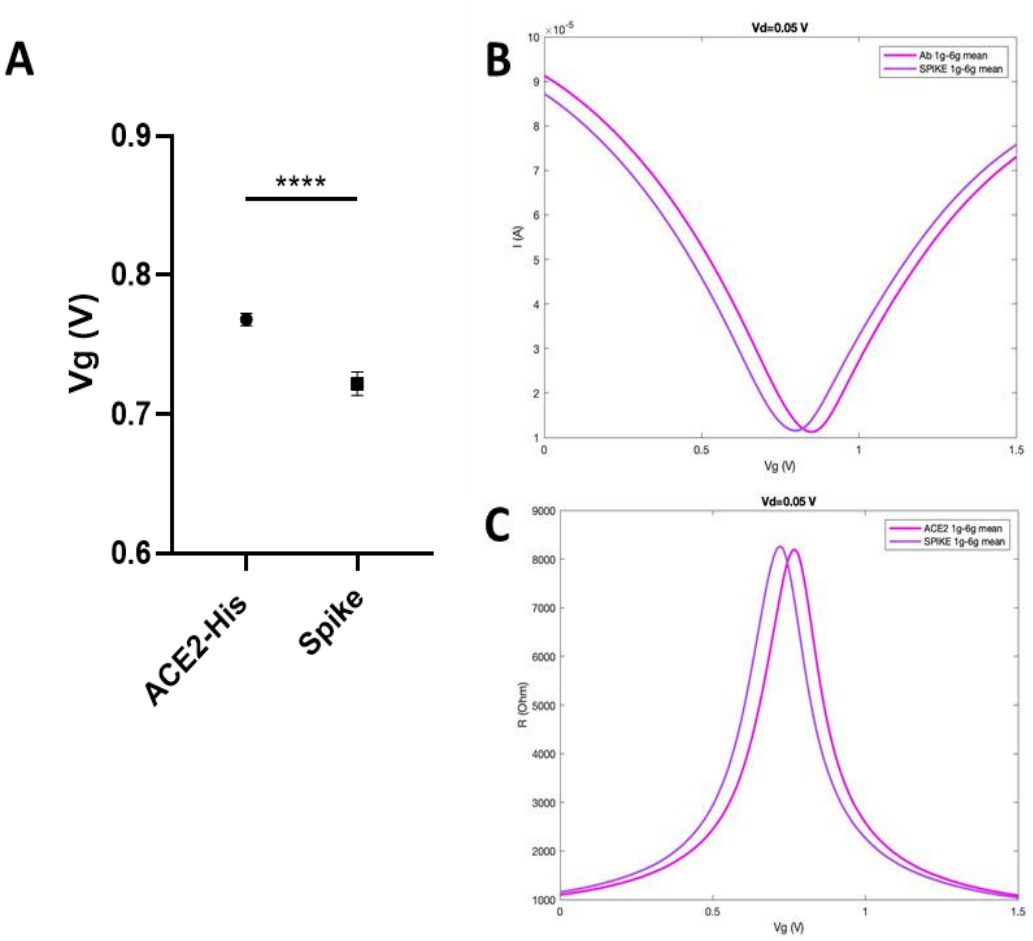

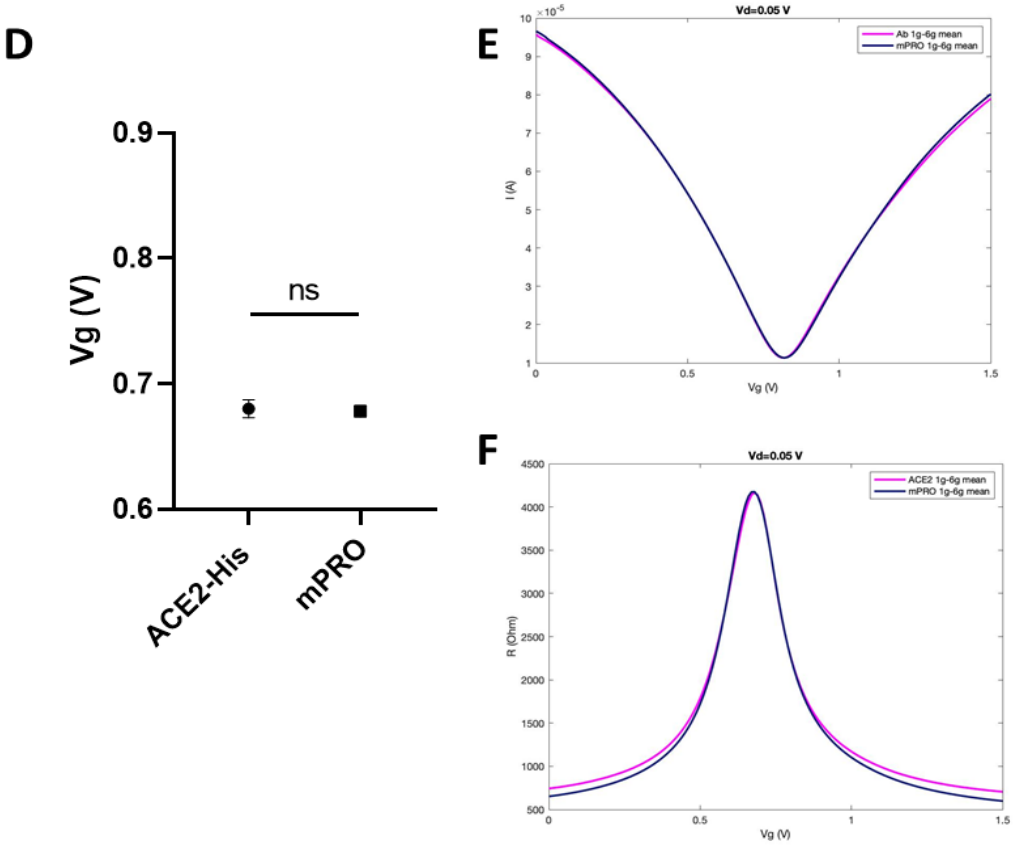

(Figure 9) (A and D) Difference in gate Voltage (V) of ACE2-HIS-conjugated GFET pre and post incubation with 2µg/ml of Trimeric Spike Protein from SARS-CoV2 (A) and mPRO from SARS-CoV2 respectively (D); (B and E) I(A)-Vg(V) output curves of the ACE2-HIS-conjugated GFET before (Light purple lines) and after (Violet lines) the addition of 2µg/ml of Trimeric Spike Protein protein (B) and 2µg/ml of mPRO (E); (C and F) RΩ(D)-Vg(G) output curves of the ACE2-HIS-conjugated GFET before (Light purple lines) and after (Violet lines) the addition of 2µg/ml of Trimeric Spike Protein protein (C) and of mPRO 2µg/ml of (F); n=6, (Welch's t test).

The second experiment has been done using the antibody anti-Spike (α-Spike) as shown in a schematic representation (Figure 10).

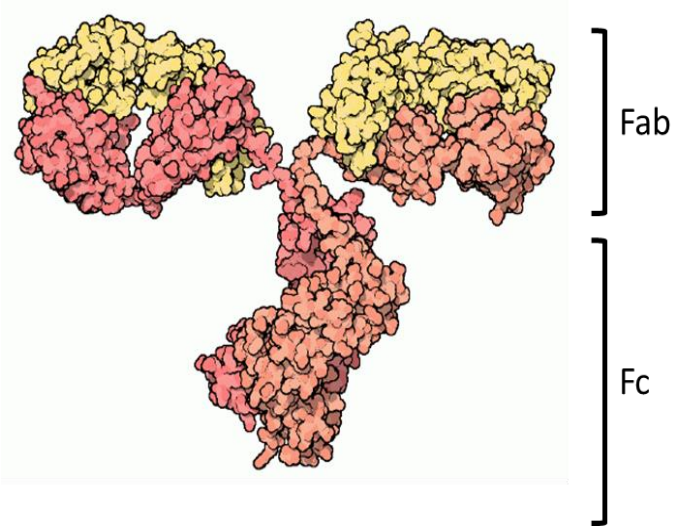

(Figure 10) Schematic representation of α-Spike used as bioreceptor

The same procedure was repeated for α-Spike; the figure 11B shows the current intensity in function of gate voltage V(g). Also in this case there is a good curve shift of α-Spike (represented in dark purple) from the blank (light purple). This curve shift can be considered as an interaction between α-Spike and Spike. In the figure 11C it is possible to observe the same curve shift, but considering the resistance (R). This represents a clear interaction between Spike and ACE-His. In the figure 11A, instead, it is represented the shift between the minimum point of V(g) in the peak (also known as Vdirac) and the blank (Spike). The same experiment has been done using mPRO as negative control (showed in the images 11 D,E,F). The figure 11D shows that there isn't any Vdirac variation between the blank and the sample.

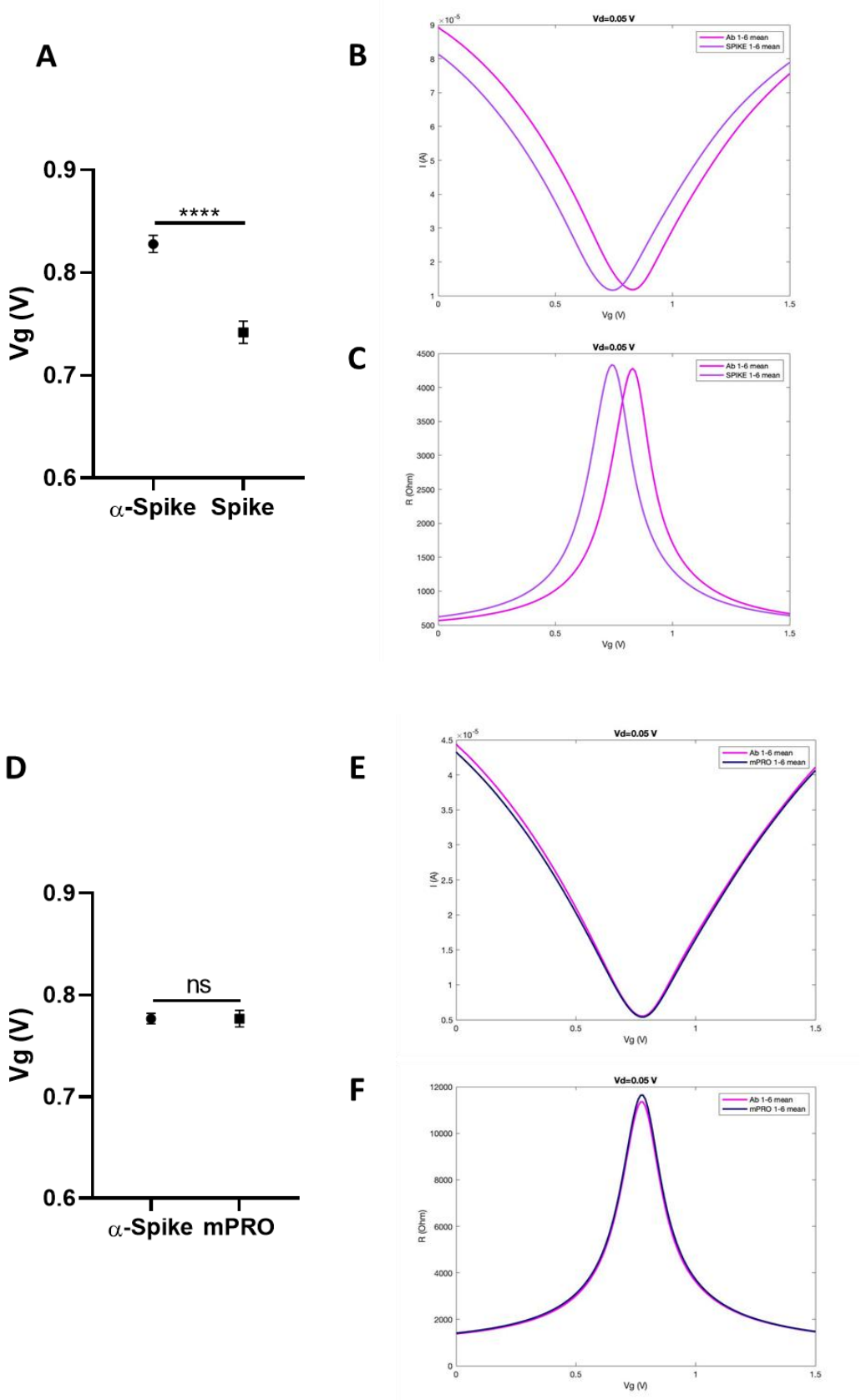
A
B
C
D
E
F
Vg (V)
0.9
0.8
0.7
0.6
****
α-Spike Spike
ns
α-Spike mPRO
Vd=0.05 V
Ab 1-6 mean
SPIKE 1-6 mean
mPRO 1-6 mean
I (A)
R (Ohm)
Vg (V)

(Figure 11) (A and D) Difference in gate Voltage (V) of α-Spike-conjugated GFET pre and post incubation with 2µg/ml of Trimeric Spike Protein from SARS-CoV2 (A) and mPROfrom SARS-CoV2 respectively (D); (B and E) I(A)-Vg(V) output curves of the α-Spike-conjugated-GFET before (Light purple lines) and after (Violet lines) the addition of 2µg/ml of Trimeric Spike Protein protein (B) and 2µg/ml of mPRO(E); (C and F) RΩ(D)-Vg(G) output curves of the α-Spike-conjugated GFET before (Light purple lines) and after (Violet lines) the addition of 2µg/ml of Trimeric Spike Protein protein (C) and 2µg/ml of mPRO (F); n=6, (Welch's t test).

For the third attempt has been used the chimeric molecule Fc-ACE2 (Figure 12)

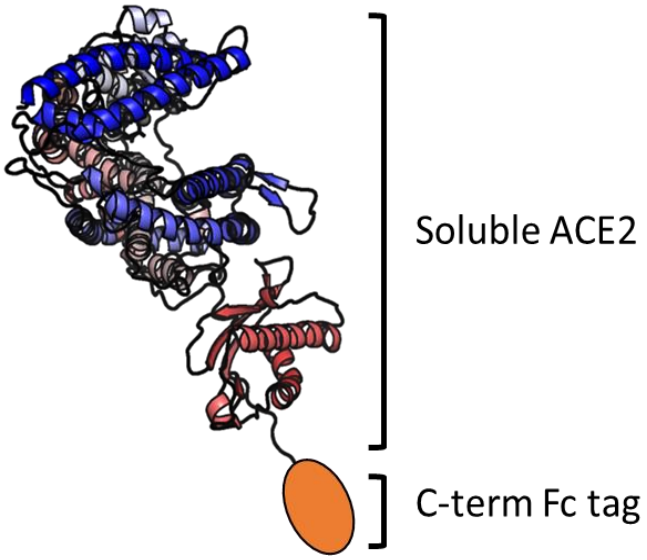

(Figure 12) Schematic representation of Fc-ACE2 used as bioreceptor.

In the figure 13B it is represented the current intensity in function of gate voltage V(g). A relevant curve shift of Spike sample (represented in dark purple) from the blank (light purple) can be observed. The curve shift observed can be considered as a clear interaction between Spike and Fc-ACE2. In the figure 13C there is the same curve shift, but considering the resistance (R) and also in this case it represents an interaction between Spike

and Fc-ACE2. In the figure 13A, instead, it is represented the shift between the minimum point of V(g) in the peak (Vdirac) and the blank (Spike). The same experiment has been done using mPRO as negative control (images 13 D,E,F). The figure 13D shows that there isn't any Vdirac variation between the blank and the sample.

A

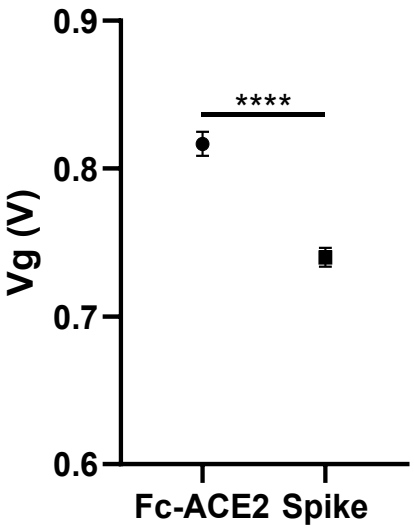

B

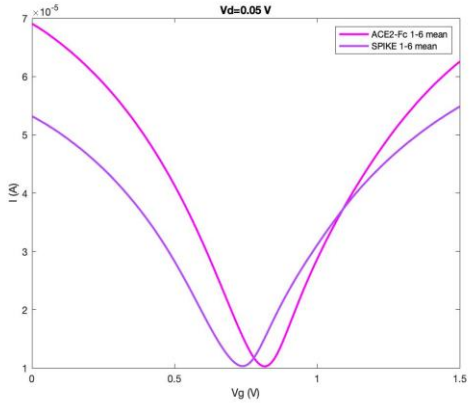

C

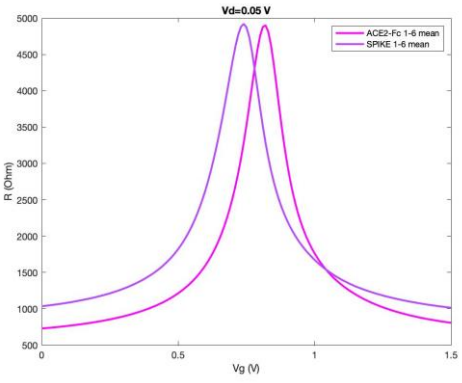

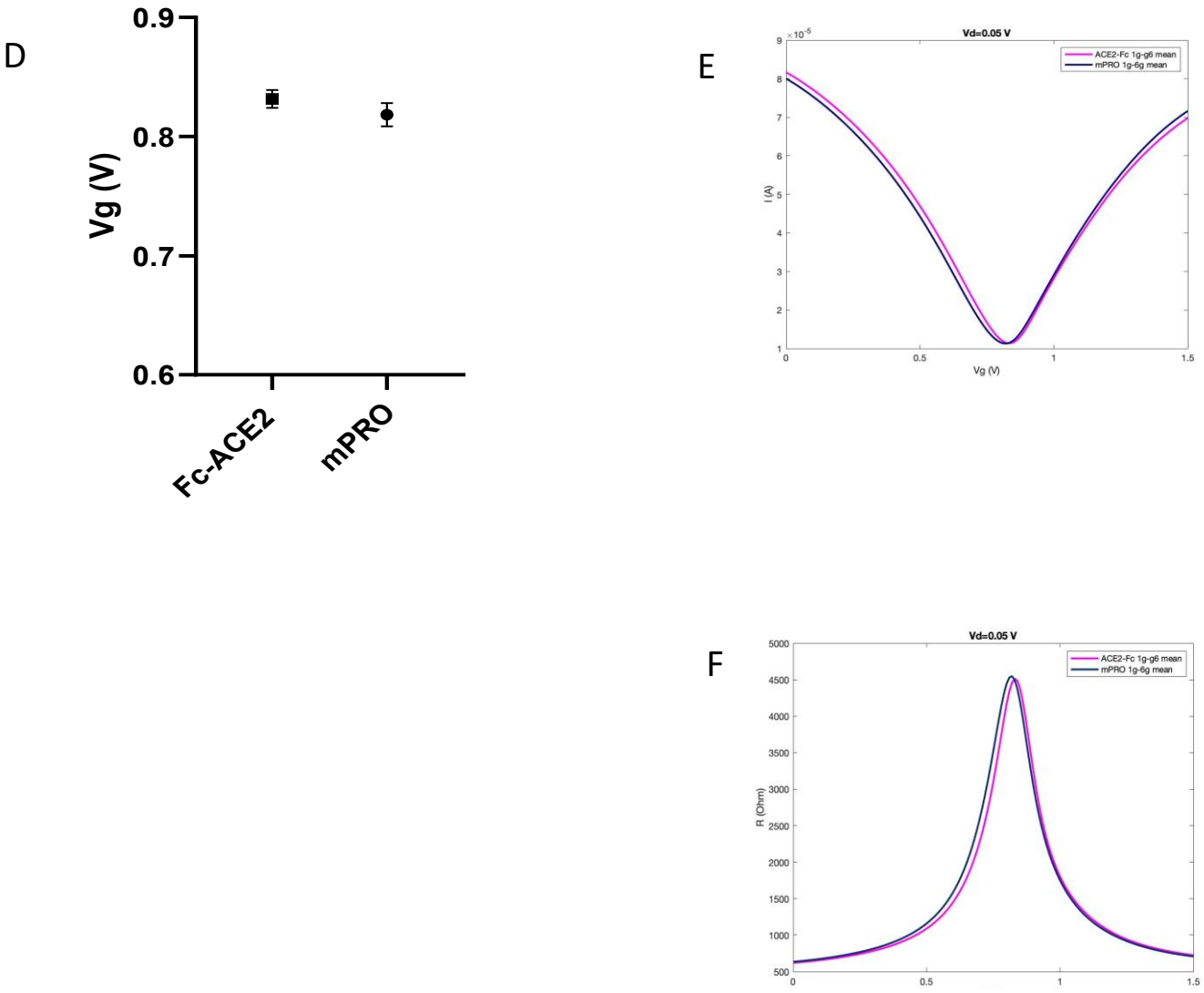

(Figura 13) (A and D) Difference in gate Voltage (V) of ACE2-Fc-conjugated GFET pre and post incubation with 2µg/ml of Trimeric Spike Protein from SARS-CoV2 (A) and mPRO from SARS-CoV2 respectively (D); (B and E)) I(A)-Vg(V) output curves of the Fc-ACE2-conjugated-GFET before (Light purple lines) and after (Violet lines) the addition of 2µg/ml of Trimeric Spike Protein protein (B) and 2µg/ml of mPRO(E); (C and F) RΩ(D)-Vg(G) output curves of the Fc-ACE2-conjugated GFET before (Light purple lines) and after (Violet lines) the addition of 2µg/ml of Trimeric Spike Protein protein (C) and 2µg/ml of mPRO (F) n=6; (Welch's t test).

2.3 Discussion about the results

The results obtained are encouraging considering all the different attempts made. It is possible to observe, from all the measurements made, the relevant signal difference in comparison to all the negative controls used and the curve shift following the RBD and ACE2 interaction.

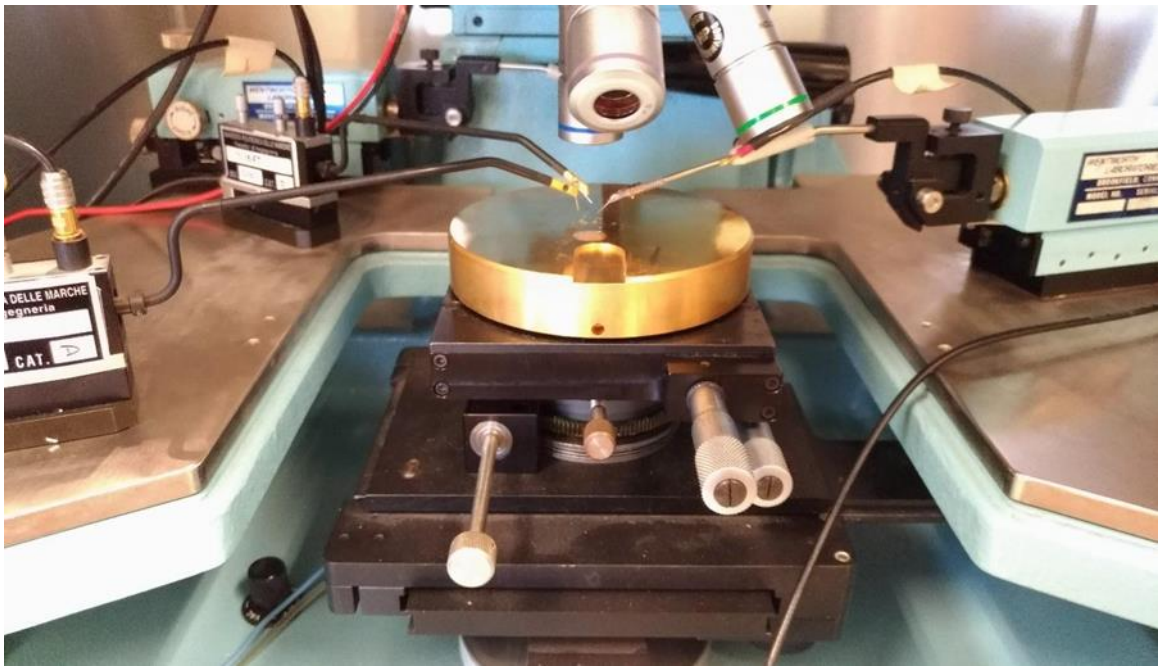

(Figure 14) (Image that shows the instrument used for the measurements in the engineering department, Università Politecnica Delle Marche)

Fc-ACE2 has shown a very promising result compared to ACE2-His and Anti-Spike. The principal reason could be the better spatial orientation of Fc-ACE2 than the other bioreceptors used during experiments. The Fc tag fused on ACE2 C-terminal forces the receptor to stay in a dimeric form. This structural obligation permits a better spatial orientation on graphene surface. The electron cloud positioned on graphene's surface is useful for the linker

binding, but at the same time it can be a problem during the ACE2 binding in the final step of graphene functionalization. This problem is due to its nature, because similarly to the linker with its aromatic chains, ACE2 can interact with its amminoacidic lateral hydrophobic chains on the graphene's surface with hydrophobic effect, π-stacking or in general with Van Der Waals interactions. On this way ACE2 can adopt an irregular position on graphene and it can't interact not only with the Spike's RBD domain, but in general it won't have the possibility to covalently bind with PBASE. This problem can be reduced, but not completely removed, with the use of chimeric molecule Fc-ACE2 because on this way, the interaction with the linker will be done with the lysines present in the Fc region of the tag; this will permit the right ACE2 spatial orientation with a consequent good interaction with Spike protein. For what concerns the kind of interactions there aren't differences between ACE2 and Fc-ACE2, but the only element who changes is the possibility to obtain a better spatial orientation with Fc-ACE2; for this reason, the results are encouraging, but also the results obtained with ACE2-His and Ab Anti-Spike (α-Spike) are really encouraging. Shift on current intensity during the measurement steps can be detectable also for these two elements; starting with the ACE2 use, there aren't differences in terms of interaction with RBD in comparison to Fc-ACE2, but what really changes is the way of

interaction with the linker because in this case is the same ACE2 that interacts with PBASE, differently from Fc-ACE2 where is the Fc element to have this task, even if the risk of a direct interaction between ACE2 and the PBASE still exists. The result is a higher risk of wrong interaction not only with the linker, but also a direct interaction between graphene and ACE2 with its amminoacidic hydrophobic chains with a consequent problem during the RBD-ACE2 interaction step. It is important to highlight, however, that a good and regular linker distribution on graphene's surface reduces this problem even if it can not solve it entirely. As it was observed, also in this case, variations during current intensities measurements are detectable and show a relevant curve shift. A different kind of analysis can be done for the use of Spike's antibody (α-Spike); this diffent analysis does not concern the results obtained, even in this case they are clear and encouraging, but it is about the different kind of interaction with Spike protein because in this case there is no more ACE2, for the interaction, but there is an antibody.This is, anyway, a highly specific interaction and it can be confirmed, with high reliability, that the curve shift is due to the effective interaction between Spike and its antibody considering that, of course, this antibody won't bind to the negative control used, mPRO.

Chapter three

MATERIALS AND METHODS

3.1 GFET preparation for functionalization step

GFET functionalization is a long process and it is the basis for the entire experiment. It is important to understand that the GFET functionalization step is a process that can vary according to the linker used. In these experiments, we have used PBASE. The nature of linker itself, with its chemical-physical properties, has a key role for the determination of the solvent needed as medium for its dissolution. DMF was used as solvent according to the manufacturer's protocol (Figure 14). The PBASE concentration in DMF was 5mM, obtained with 1mg of PBASE's dust dissolved in 500 uL of DMF; for these experiments were utilized only 25 µL of the initial 500 µL prepared. For a better dissolution of casually formed PBASE aggregates in the DMF, it has been used a sonication process for 10 seconds (**Sonics Vibra Cell** ®). The

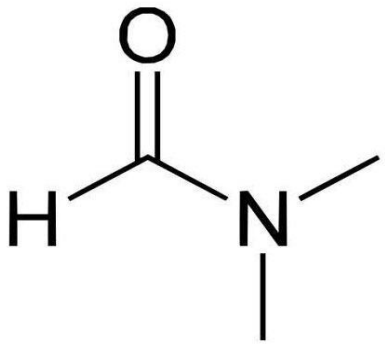

(Figure 14) (DMF chemical structure)

following step after sonication consists in the depositing of this 25 μL on chip covering all the surface trying to obtain an omogenous PBASE distribution. At the end of this process, two hours of room temperature incubation are requested. In this way the linker will bind on the graphene's surface according to what listed in the previous chapter about linker's binding on graphene. (It is strongly recommended covering the chip with silver paper to protect it from light sources).

3.2 GFET washes and remove/block of excess PBASE

Once that the two hours r.t. incubation has finished, it is important to remove the excess of PBASE on the graphene's surface and the possible irregular aggregates formed. These aggregates are formed by hydrophobic interactions, π-stacking etc. between linker molecule (differently from the regular linker and graphene's surface interaction). For this reason, three washes (1 mL each) of DMF followed by 3 washes (1 mL each) of D.I. water are needed. The chip is then dried with a slight nitrogen flow.

3.3 Final measurements

Regarding the measurements carried out, obtained based on the premises listed in the previous paragraphs, they were carried out at the Department of

Engineering (Polytechnic University of Marche). These measurements were carried out after various experiments condupted on GFET and reported below:

Protocol n°1: 24/09/2020

- 1 mg PBASE in 1 mL DMF = [2,5 mM PBASE] and 2 hours incubation at R.T.
- 3x washes with DMF (1 mL each) e 3x washes with distilled water (1 mL each).
- Drying with nitrogen flow.
- Deposition on chip 50 µL ACE2 [250 µg/mL] in PBS1X (pH 7) and O.N. incubation at 4°C.
- 3x washes with DMF (1 mL each) e 3x washes with distilled water (1 mL each).
- Drying with nitrogen flow.
- Blocking of PBASE free residue with 50 µL glycine [100 mM] in PBS1X and R.T. incubation 30 minutes.
- 3x washes with PBS1X (1 mL each) e 3x washes with distilled water (1 mL each).
- Drying with nitrogen flow.
- Add 20µL Spike Trimeric [2 µg/µL] in PBS1X on chip.

- Blank measurement with PBS1X.
- Wash with distilled water and drying
- Add 8 µL mPRO [2,5 µg/mL] in PBS1X and R.T. incubation for 15 minutes.
- Electrical measurement of six transistors.
- 3x washes with PBS 0,01X.
- Electrical measurement of twelve transistors.
- 8 µL Spike [2,5 µg/mL] in PBS 1X on first 6 transistorsand incubation 15 minutes at R.T.
- Electrical measurement of six transistors
- 3x washes with PBS 0,01X.
- Measurements of 12 transistors.
- Washes in distilled water and chip drying.
- 8 µL Spike [2,5 µg/mL] in PBS 0,01X on second 6 transistors and R.T. incubation 15 minutes.
- Measurement of second 6 transistors.
- 3x washes with PBS 0,01X.
- Measure again the 6 transitors.

Protocol n°2: 29/09/2020

- PBASE [5mM] 1mg in 500 µL DMF; withdraw 25 µL to deposit on transistor.
- 10 seconds sonication (**Sonics Vibra Cell** ®).
- R.T. incubation for 2 hours.
- 3x washes with DMF (1 mL each) e 3x washes with distilled water (1 mL each).
- Drying with nitrogen flow.
- 20 µL ACE2 [250 µg/mL] in PBS 1X and incubation O.N. at 4°C.
- 3x washes with PBS1X (1mL each).
- Drying with nitrogen flow.
- 50 µL glycine [100mM] in PBS1X and R.T. incubation 30 minutes.
- 3X washes with PBS1X and then 3X washes with PBS 0,01X.
- Drying with nitrogen flow.
- Blank measurement with PBS 0,01X.
- 3x with PBS 0,01X (1 mL each).
- Add 20 µL Spike [2,5µg/mL] in PBS 0,01X.
- R.T. incubation 15 minutes.
- 3x washes (3 mL each) (measure after every single washing step).
- 20 µL of PBS 0,01X (before every measure).

Protocol n°3: 1-10-2020 / 2-10-2020

- Prepare **2** chip for the use.
- PBASE [5mM], 1 mg in 500 µL DMF; withdraw for the use only 25 µL.
- 10 seconds sonication.
- R.T. incubation 2 hours.
- 3x washes with DMF (1 mL each) e 3x washes with distilled water (1 mL each).
- Drying with nitrogen flow.
- Add 50 µL of ACE2 [250 µg/mL].
- 6x washes with PBS1X (1 mL each).
- 20 µL of PBS1X to use as blank.
- 2x washes (5 mL each) of PBS1X and 1x wash (1mL) with distilled water and then again 20 µL of PBS1X (measure after every wash step).
- Add 20 µL of Spike [2,5 µg/mL] in PBS1X on chip #1.
- Add 20 µL of mPRO [2 µg/mL] in PBS1X on chip #2.
- 1x final wash (10 mL) of PBS 1X and 1x wash (1mL) follwed by final measurement.

Protocol n°4: 6-10-2020 / 7-10-2020

- Prepare for the use **2** chip.
- pBase [5mM], 1 mg in 500 µL of DMF; withdraw for the use only 25µL.
- 10 seconds sonication (**Sonics Vibra Cell** ®).
- R.T. incubation 2 hours.
- 3x washes with DMF (1 mL each) e 3x washes with distilled water (1 mL each).
- Drying with nitrogen flow.
- Add 50 µL of solution containing 12,5 µL of Ab anti-Spike [250 µg/mL] and 37,5 µL of PBS1X followed by incubation O.N. a 4°C.
- R.T. stabilization 30 minutes.
- 6x washes with PBS1X (1 mL each).
- 20 µL of PBS1X to use as blank.
- 2x washes (5 mL each) of PBS1X and 1x wash (1mL) with distilled water and then again 20 µL of PBS1X (measure after every wash step).
- Add 20 µL of Spike [2,5 µg/mL] in PBS1X on chip #1.
- Add 20 µL of mPRO [2 µg/mL] in PBS1X on chip #2.
- 1x final wash (10 mL) of PBS 1X and 1x wash (1 mL) of distilled water followed by final measurement.

Protocol n°5: 8-10-2020 / 9-10-2020

- PBASE [5mM], 1 mg in 500 µL of DMF; withdraw for the use only 25µL.
- 10 seconds sonication (**Sonics Vibra Cell** ®).
- 2 hours R.T. incubation.
- 3x washes with DMF (1 mL each) e 3x washes with distilled water (1 mL each).
- Drying with nitrogen flow.
- Add 50 µL of solution containing 31 µL of Fc-ACE2 [0,25 mg/mL] and 19µL of distilled water followed by O.N. incubation at 4°C.
- R.T. stabilization 30 minutes.
- 6x washes with PBS1X (1 mL each).
- 20 µL of PBS1X to use as blank.
- 2x washes (5 mL each) of PBS1X and 1x wash (1 mL) with distilled water and then again 20 µL of PBS1X (measure after every single wash step).
- Add 20 µL of Spike [2,5 µg/mL] in PBS1X on chip #1.

- 1x final wash (10 mL) of PBS 1X and 1x wash (1 mL) with distilled water followed by final measurement.

Dialysis Fc-ACE2: 8-10-2020

- Withdraw 350 µL Fc-ACE2 [1,16 mg/mL] (mantained at -20°C). (The initial medium with Fc-ACE2 contains 20 mM TRIS-HCl, 300 mM NaCl, 1 mM ZnCl2, 10% glycerol).
- Take a concentrator "**Amicon®-Ultra-4**".
- Perform the first centrifugation step (15 minutes) in water at 400 rpm, rotor name "**Beckman SX 4400"**.
- Add 350 µL Fc-ACE2 [1,16 mg/mL] and 3,15 mL PBS1X to begin the dialysis.
- Peform the first centrifugation for 10 minutes (350µL total volume residue [2mM TRIS-HCl]).
- Add 3,15 mL of PBS1X and repeate the 10 minutes centrifugation step (400 µL of total solution volume residue [0,2 mM TRIS-HCl]).
- Add 3mL PBS1X and centrifuge other 10 minutes [0,02 mM TRIS-HCl].

Chapter four

Future perspective

4.1 Advantages on the GFET use for SARS-CoV-2 detection

There are many advantages about the application of this biotechnological tool in a biological and medical contest. Firstly, the response rapidity in the obtaining of the result, is one of the greatest advantages in the actual pandemic contest. The rapid and large-scale identification of SARS-CoV-2 in infected individuals, will permit a more precise and specifical action against the virus. Secondly, another advantage is the use of Spike's natural target (ACE2 for a more concise and specific detection. This entire system can also be improved considering not only the high heterogeneity in the experiment set up, but also in the molecular target choice. For this reason, many attempts have been done not only using ACE2-His (that showed good results), but also using for example, the anti-Spike antibody (α-Spike) and the chimeric protein Fc-ACE2. In this way relevant alternatives have been tried, starting from the "basic protocol", characterized by using ACE2. Every target has its own characteristics, and this helped to a better understanding of which protocol could be the best option. As third, another relevant advantage is the possibility to reuse the same chip for several patients; this is possible by performing various washes steps after ever single application, for the residue's removal

from the chip. This aspect will permit to analize several patients in a short time with one single chip and with a substantial saving of money. The possibility to analize a bigger number of patients means that there will be a larger scale screening activity in the population limiting on this way, the SARS-CoV-2 diffusion. This also makes possible acting promptly towards infected individuals. It isn't just a case that this kind of detection system has been applied not only for SARS-CoV-2 or medical applications, but also in different contexts. The set up of a standard protocol for the GFET use is a very important goal that can be continuosly improved starting from the linker binding step to the functionalization step. For this reason, different alternatives for the functionalization step have been considered. There is another aspect to improve and regards the washing steps. This step has the task of removing ever single element that may affect the subsequent measurement. Moreover, it is possible to say that the use of GFET for SARS-CoV-2 detection is really useful under many aspects, in particular considering the various improving possibility that have been considered before. This could make this system more efficient in comparison to other alternatives.

4.2 Advantages on GFET production with a lipid film

A key point on SARS-CoV-2 detection with GFETs results is the use of ACE2, to recognize Spike, in particular the RBD domain. For this reason, it is important a correct functionalization of graphene surface because it will give a correct ACE2 spatial orientation on its surface and a consequent good interaction with the RBD domain. The main risk is that ACE2 could have a bad spatial orientation on graphene's surface. There are many options to solve this problem; it is possible to use the chimeric molecule Fc-ACE2 (with good results), as it was reported before, but another suggesting option is the production of a lipid film that covers the graphene's surface. This method has been used and tested in recent bibliography and not only for a medical application (41) (42). This particular application gives the possibility to create with high fidelity the ACE2's *natural environment* because it is an integral membrane receptor. Another related advantage consists in the possibility to clone, on this way, the entire ACE2 protein with its transmembrane helix; without a lipid film ACE2 must be cloned whithout this elix. The main advantage is that this lipid film can be produced using in the lipid mix the dipalmitoylphosphatidylcholine (DPPC) (43) that is a well-known pulmonary surfactant; it makes this lipid film highly similar to the ACE2 *natural environment*. This system will lead to a *natural folding* of ACE2 with its transmembrane inside this lipid film. This kind of technology based on a lipid

film has been used in different and various context with good results, for example, the saxitoxin detection that is a soluble toxin produced by flagellate protists. The resuls obtained were excellent, considering the fast response time (5-20 minutes) and the detection limit (1nM saxitoxin, STX) (44). Another relevant application is the use of graphene for the rapid detection of choleric toxin using a lipid film with its natural receptor, the GM1 ganglioside. Also in this context the results have shown a fast response time (5 minutes) and a detection limit of choleric toxin about 1 nM; the main relevant aspect is the high reproducibility, selectivity and specificity also considering that this biosensor has been used with samples from contaminated lake water (45). The possibility to produce a lipid film on a graphene sheet can be highly simplified with the use of anionic and neutral liposomes. This system has shown good results in the formation of a single layer membranes that partially cover the graphene's surface (46). Another important use for this kind of technology was the carbofuran detection that is a neurotoxin using its natural target emebedded in the lipid film. Also in this case the results showed an excellent response time (20 seconds) (47). Other relevant applications in the health sector were the detection of NAA (1-naphthalenacetic acid), D-Dimer and also the cholesterol detection. There are many applications of lipid films on graphene sheets and it results, in this way, a method that can

guarantee optimal results both in time and target detection limits; the application of this kind of technology also for the SARS-CoV-2 detection can play a key role considering all the advantages mentioned before. In addition, this system has been used with excellent results also for other contexts like, for example, the choleric toxin detection using its natural receptor and consequently, the same can be done for Spike and ACE2.

4.3 Advantages about the use of long apolar chains and Van Der Waals interactions as PBASE substituents

In the previous chapters the use of PBASE has already been explained with all of its advantages and disadvantages. Briefly, the use of hydrophobic interactions, π-stacking and in general, Van Der Waals interactions doesn't involve the formation of covalent bonds and consequently it won't be possible anchor the PBASE on graphene's surface. This means that the linker won't assume a fixed position on graphene's surface and PBASE will fluctuate on the electron cloud. This aspect can lead to the formation of linker irregular agglomerates and a bad distribution on the surface with the risk of compromising the entire functionalization process and in general, the entire experiment. The possibility to use long apolar chains and not a linker with its aromatic chains seems a good option to solve this problem. It is important to highlight that also in this case it won't be possible to covalently anchor the

linker on graphene's surface, but with this system the binding strength between the apolar chains and the electron cloud will increase proportionally to the length and the dimension of the chain. More specifically the key aspect is the application of London dispersion forces and hydrophobic effects between the graphene's surface and the apolar chains. The principal advanatge is the possibility to obtain, in this way, a linker anchored in a better way than the PBASE and also a regular and specifical linker distribution on graphene's surface. This will also solve the problem of the direct interaction between ACE2 and the electron cloud because with this system is possible to cover more evenly and regular the graphene's surface than the PBASE. There are many advantages using this method because it is possible to cover the graphene's surface with a "*carpet like"* system. An important consideration is that also the long apolar chains in a regular and homogeneous distance could stabilize themselves with stabilizing interactions between the apolar chains, similarly to what happens between the graphene's surface and this apolar chains. With this method it is possible to produce a more stable system than PBASE and a regular distribution of linker on graphene's surface and consequently, ACE2. This will lead to a better interaction with Spike (48) (49) (50) (51) (52) (53). In conclusion, considering the different aspects listed

in the previous chapters, this system will make the whole process more efficient for the SARS-CoV-2 detection using GFETs.

Bibliography

(1) Zhu, N. et al. A Novel Coronavirus from patients with pneumonia in China, 2019. N. Engl. J. Med. 382, 727–733 (2020).

(2) Gralinski, L. E. & Menachery, V. D. Return of the coronavirus: 2019-nCoV. Viruses 12, 135 (2020).

(3) Jiang, S., Du, L. & Shi, Z. An emerging coronavirus causing pneumonia outbreak in Wuhan, China: calling for developing therapeutic and prophylactic strategies. Emerg. Microbes Infect. 9, 275–277 (2020).

(4) Woo PC, Lau SK, Huang Y, Yuen KY. Coronavirus diversity, phylogeny and interspecies jumping. Exp Biol Med (Maywood). 2009; 234:1117–27 10.3181/0903-MR-94

(5) Lu, R. et al. Genomic characterisation and epidemiology of 2019 novel coronavirus: implications for virus origins and receptor binding. Lancet 395, 565–574 (2020).

(6) Chan, J. F. et al. Genomic characterization of the 2019 novel human-pathogenic coronavirus isolated from a patient with atypical pneumonia after visiting Wuhan. Emerg. Microbes Infect. 9, 221–236 (2020).

(7) Zhou, P. et al. A pneumonia outbreak associated with a new coronavirus of probable bat origin. Nature 579, 270–273 (2020).

(8) Lu, R. et al. Genomic characterisation and epidemiology of 2019 novel coronavirus: implications for virus origins and receptor binding. Lancet 395, 565–574 (2020).

(9) Zhou, P. et al. A pneumonia outbreak associated with a new coronavirus of probable bat origin. Nature 579, 270–273 (2020).

(10) Anderson, K. G., Rambaut, A., Lipkin, W. I., Holmes, E. C. & Garry, R. F. The proximal origin of SARS-CoV-2. Nat. Med. 26, 450–452 (2020).

(11) Zhou, P. et al. A pneumonia outbreak associated with a new coronavirus of probable bat origin. Nature 579, 270–273 (2020).

(12) Hoffmann, M. et al. SARS-CoV-2 cell entry depends on ACE2 and TMPRSS2 and is blocked by a clinically proven protease inhibitor. Cell 181, 271–280 (2020).

(13) Shang, J. et al. Structural basis of receptor recognition by SARS-CoV-2. Nature 581, 221–224 (2020).

(14) Walls, A. C. et al. Structure, function, and antigenicity of the SARS-CoV-2 spike glycoprotein. Cell 181, 281–292 (2020).

(15) Wan, Y., Shang, J., Graham, R., Baric, R. S. & Li, F. Receptor recognition by the novel coronavirus from Wuhan: an analysis based on decade-long structural studies of SARS coronavirus. J. Virol. 94, e00127-20 (2020).

(16) Shang, J. et al. Structural basis of receptor recognition by SARS-CoV-2. Nature 581, 221–224 (2020).

(17) Shang, J. et al. Structural basis of receptor recognition by SARS-CoV-2. Nature 581, 221–224 (2020).

(18) Shang, J. et al. Structural basis of receptor recognition by SARS-CoV-2. Nature 581, 221–224 (2020).

(19) Wan, Y., Shang, J., Graham, R., Baric, R. S. & Li, F. Receptor recognition by the novel coronavirus from Wuhan: an analysis based on decade-long structural studies of SARS coronavirus. J. Virol. 94, e00127-20 (2020).

(20) Letko, M., Marzi, A. & Munster, V. Functional assessment of cell entry and receptor usage for SARS-CoV-2 and other lineage B betacoronaviruses. Nat. Microbiol. 5, 562–569 (2020).

(21) Gui, M. et al. Cryo-electron microscopy structures of the SARS-CoV spike glycoprotein reveal a prerequisite conformational state for receptor binding. Cell Res. 27, 119–129 (2017).

(22) Song, W., Gui, M., Wang, X. & Xiang, Y. Cryo-EM structure of the SARS coronavirus spike glycoprotein in complex with its host cell receptor ACE2. PLoS Pathog. 14, e1007236 (2018).

(23) Kirchdoerfer, R. N. et al. Stabilized coronavirus spikes are resistant to conformational changes induced by receptor recognition or proteolysis. Sci. Rep. 8, 15701 (2018).

(24) Yuan, Y. et al. Cryo-EM structures of MERS-CoV and SARS-CoV spike glycoproteins reveal the dynamic receptor binding domains. Nat. Commun. 8, 15092 (2017).

(25) Walls, A. C. et al. Structure, function, and antigenicity of the SARS-CoV-2 spike glycoprotein. Cell (2020).

(26) Tian, X. et al. Potent binding of 2019 novel coronavirus spike protein by a SARS coronavirus-specific human monoclonal antibody. Emerg. Microbes Infect. 9, 382–385 (2020).

(27) Zhou, P. et al. A pneumonia outbreak associated with a new coronavirus of probable bat origin. Nature 579, 270–273 (2020).

(28) Tortorici, M. A. & Veesler, D. Structural insights into coronavirus entry. Adv. Virus Res. 105, 93–116 (2019).

(29) Li, F. Structure, function, and evolution of coronavirus spike proteins. Annu. Rev. Virol. 3, 237–261 (2016).

(30) Letko, M., Marzi, A. & Munster, V. Functional assessment of cell entry and receptor usage for SARS-CoV-2 and other lineage B betacoronaviruses. Nat. Microbiol. 5, 562–569 (2020). First functional assessment of the interaction of the SARS-CoV-2 Spike protein receptor binding domain with the cellular receptor ACE2.

(31) Technical datasheet (Graphene field-effect transistor chip: S-20, Graphenea®)

(32) Measurement protocols and handling instructions (Graphene field-effect transistor chip: GFET-S20, Graphenea®).

(33) Stephanos Karapetis, Georgia-Paraskevi Nikoleli, Christina G.Siontorou , Dimitros P.Nikolelis, Nikolaos Tzamtzis , Nikolas Psaurodakis, Electroanalysis.

(34) Spyridoula Bratakou, Georgia-Paraskevi Nikoleli, Dimitros P.Nikolelis, Nikolas Psaurodakis, Electroanalysis.

(35) Song L, Hobaugh MR, Shustak C, Cheley S, Bayley H, Gouaux JE. Structure of staphylococcal alpha-hemolysin, a heptameric transmembrane pore. Science.

(36) Aksimentiev A, SchultenImaging alpha-hemolysin with molecular dynamics: ionic conductance, osmotic permeability, and the electrostatic potential map. Byophisical journal.

(37) Prinjaporn Teengama, Weena Siangproh, Adisorn Tuantranont, Charles S.Henry, Tirayut Vilaivane, Orawon Chailapaku) – Analytica chimica acta

(38) Goodwin AP, Tabakman SM, Welsher K, Sherlock SP, Prencipe G, Dai H). Phospholipid-dextran with a single coupling point: a useful amphiphile for functionalization of nanomaterials – ACS Publications

(39) Nikolelis, D.P.; Ntanos, N.; Nikoleli, G.-P.; Tampouris, K. Development of an Electrochemical Biosensor for the Rapid Detection of Naphthalene Acetic Acid in Fruits by Using Air Stable Lipid Films with Incorporated Auxin-Binding Protein 1 Receptor. Protein Pept. Lett. 2008, 15, 789–794.

(40) Marica Marrese ,Vincenzo Guarino , Luigi Ambrosio. Atomic Force Microscopy: A Powerful Tool to Address Scaffold Design in Tissue Engineering – MDPI

(41) Spyridoula Bratakou, Stephanos Karapetis, Georgia-Paraskevi Nikoleli, Christina G.Siontorou , Dimitros P.Nikolelis, Nikolaos Tzamtzis , Nikolas Psaurodakis) Development of an Electrochemical Biosensor for the Rapid Detection of Cholera Toxin Based on Air Stable Lipid Films with Incorporated Ganglioside GM1 Using Graphene Electrodes. Electroanalysis

42) Nikolelis, D.P.; Chaloulakos, T.-I.; Nikoleli, G.-P.; Psaroudakis, N. A portable sensor for the rapid detection of naphthalene acetic acid in fruits and vegetables using stabilized in air lipid films with incorporated auxin-binding protein 1 receptor. Talanta 2008, 77, 786–792.

43) Nikolelis, D.P.; Ntanos, N.; Nikoleli, G.-P.; Tampouris, K. Development of an Electrochemical Biosensor for the Rapid Detection of Naphthalene Acetic Acid in Fruits by Using Air Stable Lipid Films with Incorporated Auxin-Binding Protein 1 Receptor. Protein Pept. Lett. 2008, 15, 789–794.

(44) Jiyang Liu, Shaojun Guo, Lei Han, Tiansu Wang, Wei Hong, Yaqing Liu and Erkang Wang Synthesis of phospholipid monolayer membrane functionalized graphene for drug delivery. Journal of materials chemistry

(45) Spyridoula Bratakou, Georgia-Paraskevi Nikoleli, Dimitros P.Nikolelis, Nikolas Psaurodakis Development of a Potentiometric Chemical

Sensor for the Rapid Detection of Carbofuran Based on Air Stable Lipid Films with Incorporated Calix[4]arene Phosphoryl Receptor Using Graphene Electrode. Electroanalysis

46) Spyridoula Bratakou, Georgia-Paraskevi Nikoleli, Christina G.Siontorou, Dimitros P.Nikolelis, Stephanos Karapetis, Nikolas Tzamtzis.Development of an Electrochemical Biosensor for the Rapid Detection of Saxitoxin Based on Air Stable Lipid Films with Incorporated Anti-STX Using Graphene Electrodes. Electroanalysis

47) Spyridoula Bratakou, Stephanos Karapetis, Georgia-Paraskevi Nikoleli, Christina G.Siontorou , Dimitros P.Nikolelis, Nikolaos Tzamtzis , Nikolas Psaurodakis) Development of an Electrochemical Biosensor for the Rapid Detection of Cholera Toxin Based on Air Stable Lipid Films with Incorporated Ganglioside GM1 Using Graphene Electrodes. Electroanalysis

(48) Wu, Y.; Hudson, J. S.; Lu, Q.; Moore, J. M.; Mount, A. S.; Rao,A. M.; Alexov, E.; Ke, P. C. J. Phys. Chem. B 2006, 110, 2475. (b)Tasis, D.; Papagelis, K.; Douroumis, D.; Smith, J. R.; Bouropoulos,N.; Fatouros, D. G. J. Nanosci. Nanotechnol. 2008, 8, 420.

(49) Shi Kam, N. W.; O'Connell, M.; Wisdom, J. A.; Dai, H. Proc. Natl.Acad. Sci. U.S.A. 2005, 102, 11600

(50) (a) Shi Kam, N. W.; Liu, Z.; Dai, H. J. Am. Chem. Soc. 2005, 127,12492. (b) Liu, Z.; Winters, M.; Holodniy, M.; Dai, H. Angew. Chem.,Int. Ed. 2007, 46, 2023.

(51) Liu, Z.; Cai, W.; He, L.; Nakayama, N.; Chen, K.; Sun, X.; Chen,X.; Dai, H. Nat. Nanotechnol. 2007, 2, 47

(52) (a) Feazell, R. P.; Nakayama-Ratchford, N.; Dai, H.; Lippard, S. J.J. Am. Chem. Soc. 2007, 129, 8438. (b) Liu, Z.; Sun, X.; NakayamaRatchford, N.; Dai, H. ACS Nano 2007, 1, 50.

(53) De La Zerda, A.; Zavaleta, C.; Keren, S.; Vaithilingam, S.;Bodapati, S.; Liu, Z.; Levi, J.; Smith, B. R.; Ma, T.-J.; Oralkan, O.;Cheng, Z.; Chen, X.; Dai, H.; Khuri-Yakub, B. T.; Gambhir, S. S.Nat. Nanotechnol. 2008, 3, 557. (b) Welsher, K.; Liu, Z.; Daranciang,D.; Dai, H. Nano Lett. 2008, 8, 586. (c) Goodwin, A. P.; Tabakman,S. M.; Welsher, K.; Sherlock, S. P.; Prencipe, G.; Dai, H. J. Am.Chem. Soc. 2009, 131, 289.